



HAL
open science

Use of a digital image correlation method for full-field shrinkage measurement in injection molding

Antoine Dupuis, Jean-Jacques Pesce, Jean-Baptiste Marijon, Stéphane Roux,
Gilles Régnier

► **To cite this version:**

Antoine Dupuis, Jean-Jacques Pesce, Jean-Baptiste Marijon, Stéphane Roux, Gilles Régnier. Use of a digital image correlation method for full-field shrinkage measurement in injection molding. *Journal of Strain Analysis for Engineering Design*, 2022, 57 (8), pp.702-713. 10.1177/03093247211060215 . hal-04073104

HAL Id: hal-04073104

<https://hal.science/hal-04073104v1>

Submitted on 18 Apr 2023

HAL is a multi-disciplinary open access archive for the deposit and dissemination of scientific research documents, whether they are published or not. The documents may come from teaching and research institutions in France or abroad, or from public or private research centers.

L'archive ouverte pluridisciplinaire **HAL**, est destinée au dépôt et à la diffusion de documents scientifiques de niveau recherche, publiés ou non, émanant des établissements d'enseignement et de recherche français ou étrangers, des laboratoires publics ou privés.

Use of a digital image correlation method for full-field shrinkage measurement in injection molding

Antoine Dupuis^{1,2} , Jean-Jacques Pesce², Jean-Baptiste Marijon¹ ,
Stéphane Roux³  and Gilles Régnier¹ 

Abstract

An original methodology using Digital Image Correlation (DIC) has been designed to precisely measure full-field shrinkages of injection molded polymer plates and then to give the opportunity to compare quantitatively extensive numerical simulations to experiments. The principle of the methodology is based on the full-field strain determination between a reference image of the mold and that of injection-molded parts, which are $275 \times 100 \times 2.2 \text{ mm}^3$ plates. To allow for DIC calculation, $50 \mu\text{m}$ -depth engravings were machined by electro-discharge process at the surface of the mold. The result of the analysis is a 2D full-field shrinkage map over the whole plate surface (i.e. flow and transverse), with a standard deviation of 0.03%. The marking density has been shown to have a roughly linear influence on the precision of shrinkage measurement. This methodology allows the quantification of the effect of several injection parameters on in-plane shrinkage fields: holding pressure, injection flow rate and direction, geometry of injection gates, or geometrical constraints. Once the best set of parameters of material constitutive laws is identified for the simulation of polymer plates, the simulation procedure is ready to be applied on more complex 3D geometries.

Keywords

Digital Image Correlation (DIC), injection molding, shrinkage measurement, in-plane shrinkage, constrained shrinkage

Date received: 25 May 2021; accepted: 27 October 2021

Introduction

In many industrial sectors, the design of injection molds for engineering manufactured parts, as door or instrument panels for automotive industry, is difficult when an accurate shape and size of the molded part is sought and corresponds to a very expensive phase of the development project. In this context, a simulation of injection molding process is highly beneficial to estimate the parts final dimensions and supply preliminary information on mold design and injection parameters.¹

For injection molding process, many researchers reported the main injection parameters affecting the overall shrinkage: cooling time, packing pressure,^{2,3} melt temperature,⁴ injection flow rate,⁵ or mold deflection.⁶ Studying the effect of some injection parameters on the variation in local microstructure and shrinkage seems essential. Indeed, due to the high polymer viscosity and its temperature dependence, the pressure in the cavity depends on the distance from the gate,⁷ the thickness, the proximity of an edge and the thermal boundary conditions.⁸ For short fiber reinforced polymers,

due to the high sensitivity of fiber to the polymer flow, the distribution of fiber orientation has a crucial impact on shrinkage anisotropy.⁹ This anisotropy combined with the non-uniformity of in-plane shrinkages lead to warpage,¹ which is a critical issue in the industry for parts assembly.

To understand the influence of those process parameters on part dimensions and warpages, it is valuable to study the case of parts with simple shapes like plates, for which polymer flow is not very complex. In the literature, two papers have considered non-standardized

¹PIMM laboratory, Arts et Métiers Institute of Technology, CNRS, Cnam, HESAM Université, Paris, France

²Faurecia Interior Systems, Méru, France

³Laboratoire de Mécanique et Technologie, Université Paris-Saclay, ENS-Paris-Saclay, CNRS, Cachan Cedex, France

Corresponding author:

Gilles Régnier, PIMM, Arts et Métiers Institute of Technology, CNRS, Cnam, HESAM Université, 151 boulevard de l'Hôpital, Paris 75013, France.

Email: gilles.regnier@ensam.eu

approaches for the measurement of in-plane shrinkages. First, Régnier and Trotignon¹⁰ manufactured a square mold with 30 μm deep engraving lines. To determine the local anisotropic shrinkage, the distances between two lines on the mold and those imprinted on the polymer plate are measured using a microscope, coupled with a CCD camera and a precision in-plane translation stage.¹⁰ The estimated standard deviation for a local shrinkage (strain) measurement is 0.0175%. The main limiting factor of the method is the duration of the measuring procedure: fifty minutes work for one operator is required to complete the measurement of 25 local in-plane shrinkages. Later, Jansen¹¹ used a similar procedure with a grid applied on the fixed mold halves of a rectangular plate mold. A minimum measured distance of 30 mm had to be considered to limit the shrinkage measurement error, estimated to 0.06% for this study. Pomerleau and Sanschagrin⁵ proposed shrinkage measurement on circular arc-shaped engravings with the use of a profilometer. These authors called attention to the measurement errors caused by straightness imperfections of the engravings on the injected parts and by plate warpage, inducing out-of-plane shrinkage measurement. In another study, to assess the complete evolution of shrinkage from the instant of first solidification in the mold, a strain gauge was used.³ The authors were able to demonstrate that the shrinkage onset was delayed by increasing the holding pressure and that the as-molded shrinkage was reduced by the presence of geometrical constraints inside the mold. Although this technique is useful to observe the shrinkage during the whole injection cycle, it only provides one local information and the gauge itself can perturb the measurement. Lastly, other researchers chose to measure the edges of the injected samples as a way to assess shrinkage, either by width shrinkage measurement,¹² or by using a multi-sensor coordinate measuring machine.¹³

In the recent years, researchers showed a growing interest toward Digital Image Correlation techniques (DIC) for the determination of in-plane displacement or deformation field. The technique was first used to measure kinematic strain field during mechanical testing.^{14–16} Integrated approaches were later developed, comparing the displacement field resulting from FE numerical simulation¹⁷ or from experimental tests¹⁸ with the full-field measurement from DIC to assess and optimize for example materials constitutive laws. DIC technique was also used to study the induced displacement field during molding process with the identification of the effects of stiction and thermal gradient in the molten polymer on shrinkage strain.¹⁹ This technique was also used to measure shrinkage induced by chemical or thermal treatments, typically in medical industry for the study of dental composite shrinkage.^{20,21} This technique was used to measure the in-situ cure shrinkage of a thermosetting resin^{22,23} especially to relate the chemical shrinkage, the degree of cure and the coefficient of thermal expansion. In the field of

injection molding, the DIC technique was used to detect dimensional or quality defects on product and then enabled to evaluate the sensitivity of the process setting on defects,²⁴ or to implement a methodology to optimize the settings.²⁵ For all these studies, a reference state of the material was captured in a reference image, from which the time evolution of strain was followed. Unfortunately, this is not possible for injection molded parts as the reference geometry is given by the mold. It is the purpose of the present paper to propose a methodology based on DIC that can provide a quantitative map of shrinkage on the surface of injection molded parts.

Several challenges are to be faced. First, a speckle pattern is often used in DIC so as to provide a dense field of surface details that can be tracked over time. However, the hard metallic surface of the mold does not easily allow such a marking. Second, the mold surface and that of the polymer part do not share the same contrast. Third, as only the final state (after cooling) is accessible, the displacement magnitude may become large, which constitutes a difficulty for Digital Image Correlation in contrast to a slow time evolution.¹⁵

The paper first describes a fast and robust methodology based on DIC to estimate in-plane shrinkage fields of injection molded plates. This approach gives the opportunity to compare in-plane shrinkage fields qualitatively and quantitatively for different process conditions. It also allows comparing the measured shrinkage fields and the simulated ones, giving the opportunity to correlate with numerical software and to develop efficient digital twins.

Material and methods

Processed material

The material used in this study is a heterophasic ethylene-propylene copolymer reinforced by 20% wt. hemp fibers. The Young modulus of the copolymer matrix at 23°C was measured at 1450 MPa with a standard deviation of 50 MPa, obtained with 20 measurements. The density of the copolymer was measured at 905 kg/m³ and the fusion temperature at 163°C. The thermomechanical properties of this studied biocomposite can be found in the work of Dupuis et al.²⁶

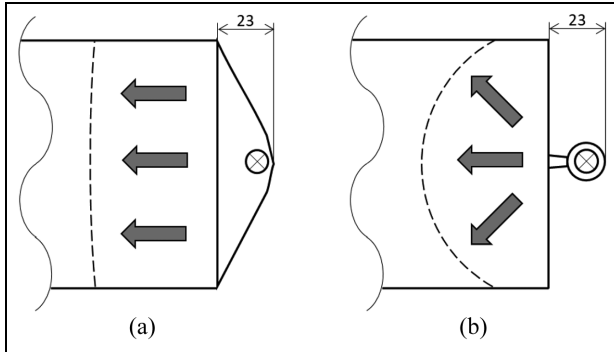
Injection molding and processing conditions

A specific plate mold equipped with a hot runner was designed and mounted on a DK Codim injection molding machine having a clamp force of 1750 kN and a screw diameter of 36 mm.

Rectangular injected plates measuring 275 \times 100 \times 2.2 mm³ were injection molded with a fan gate or a tap gate. In a previous study, Dupuis et al.²⁶ analyzed the effect of injection gate geometry and observed an effect on the fiber orientation distribution. The **fan gate** configuration with a gradual thickness reduction at its

Table 1. Injection conditions used for shrinkage field evaluation by DIC method.

Injection configuration	Mold configuration	Injection ram speed (mm/s)/ injection time (s)	Packing pressure (MPa)
Fan gate/tab gate	Simple plate/plate with ribs	30–100/2.0–0.7	0–30–40

**Figure 1.** Flow front profile with (a) fan gate geometry and (b) tab gate geometry.

center (from 2.2 to 1.5 mm) was studied to ensure a unidirectional flow front from the cavity entry (Figure 1(a)). The tab gate is more generally used in industrial mold and induces a radial flow front at the entry of the cavity (Figure 1(b)).

Some of the plates were injection molded with small peripheral ribs to block in-plane shrinkages during the cooling in the mold, promoting stress relaxation during cooling. Then, the part underwent a lower elastic spring back at ejection.

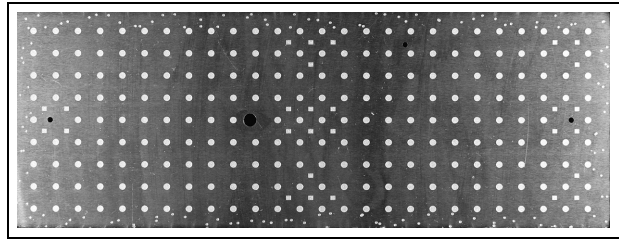
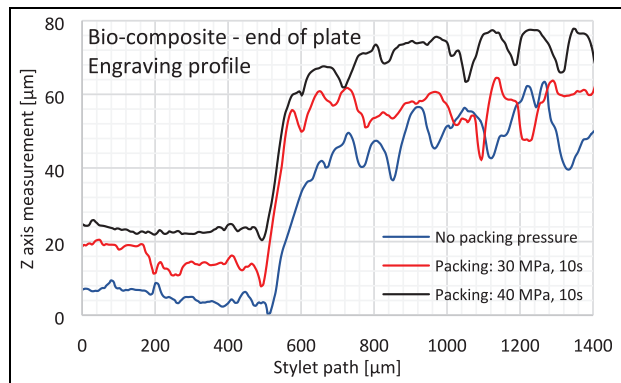
Nozzle temperature was set at 185°C and ram speed at 30 and 100 mm/s, which gave a filling time of 2.0 s and 0.71 s respectively. Nozzle pressure at switchover was about 90 MPa. For plates processed with a packing pressure phase, a constant nozzle pressure of 30 or 40 MPa was held for 10 s in hot runners by the injection ram. The cooling phase including the holding pressure phase was 35 s, with a regulation temperature for the mold set to 30°C.

The reference case of the study consists of a simple plate injected with a fan gate at a constant ram speed of 30 mm/s. At the end of filling, no packing pressure is applied, and the plate was cooled for 35 s. These injection conditions promote high shrinkage levels in flow and transverse directions and then highlight the effects of other injection conditions. Industrial parts are usually injected applying a holding pressure after the cavity filling in order to compensate for the volumetric shrinkage occurring at cooling.

The varying injection parameters considered in the paper are listed in Table 1.

Experimental setup for DIC shrinkage measurement

Engravings geometry for in-plane shrinkages measurement. To allow for the Digital Image

**Figure 2.** Mold fixed part image with engravings made by electro-discharge.**Figure 3.** Engraving profiles at end of an injected bio-composite plate depending on packing pressure level.

Correlation (DIC) technique, small engravings of 50 μm-depth were machined by electro-discharge process on the surface of fixed mold part (Figure 2). We adopted a higher roughness inside the engravings (CHARMILLE 30 grains) than in the rest of mold surface to ensure an adequate image contrast for injection molded plates. The engraving imprints are visible on the plate surface and provide patterns to be matched between injection plates images and the mold image, designated as reference. The engraving depth (Figure 3) is evaluated to be sufficient to supply a good contrast in images, even in the absence of a subsequent holding pressure. It is noteworthy to specify that the Dektak profilometer (Veeco, USA) used to obtain the measurements on plates in Figure 3 could not perform engraving measurement on the mold cavity for comparison. Nevertheless, a smaller depth should give the same results as surface roughness difference is the key point for image contrast.

Two different engravings geometries were designed on the mold surface (Figure 2). A regular distribution

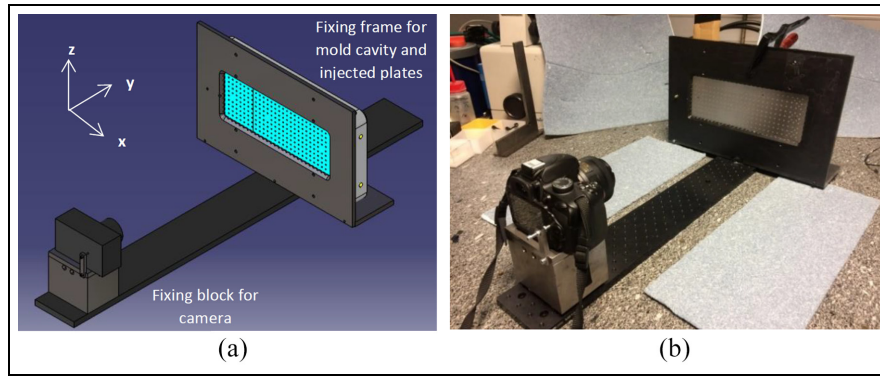


Figure 4. (a) 3D CAD view and (b) photography of the setup for image capture with removable mold cavity plate.

on the whole surface was first performed to estimate anisotropic bulk shrinkage. It consists of 3-mm-diameter disks, separated by a reference distance of 10 mm in the mold cavity. A second random distribution of 1-mm-diameter disks was added on plate edges, where DIC calculation is less precise due to poorer constraints given by neighboring pixels when displacement field regularity is used as a regularization of the problem. These 1-mm-diameter disks were evaluated as minimal for a correct templating on injection molded plate surface.

Shrinkage measurement by profilometry technique. Specific 2 mm square engravings were also located in strategic locations (cavity entry, center of the part, and near-end-of-fill region) to enable in-plane shrinkage measurements using a Dektak 150 surface profilometer from Veeco. As for regular grid of disks engraving, each pattern was separated from their neighbors by a reference distance of 10 mm both along the flow direction and transverse to it. The radius of the stylet used for the measurements was $1.5 \mu\text{m}$. A Python script was used to detect the slots of each marker and then evaluate the distance between two markers in flow and transverse direction. Due to measurement errors caused by part warpage,⁵ profilometer measurements achieved on plates without packing pressure should be considered more cautiously.

Experimental bench for plate image capture. Digital Image Correlation requires images taken in strictly identical conditions (plate position, lighting and light contrast, camera optical axis, and image resolution...). However, the mold image required a mirror symmetry before being compared to plate images. Then, a specific experimental bench was designed with a high geometrical quality. The bench was set on an optical quality marble to ensure a non-variable distance over time between camera lens and the plate at each image capture session (Figure 4). This working distance was fixed at 450 mm for all sessions. The setup is composed of an adjustable camera support to set the optical axis in a normal

direction to the plate surface, in order to minimize optical distortions for image correlation. On the other side of the bench, a frame is used to position and flatten the injected plates on 1-mm edges, using rails, avoiding position errors induced by out-of-plane deformation. The instrumentation was placed within a darkroom to ensure lighting reproducibility thanks to a LED ribbon having a low-angled lighting on plates to avoid surface reflections.

Images were taken in gray level with a NIKON D3200 and an AF-S DX NIKKOR 35 mm f/1.8 G camera lens. The original images of 6016×4000 pixels are taken in jpeg format. Before fixing the plates on the instrumentation, chalk powder was applied on part surface to enhance optical contrast between the engravings and the rest of the part (Figure 5). The camera was manually triggered for each image capture with an exposure time set at 1 s, minimizing the aperture and maximizing the depth of field. The intensity of LED ribbon lighting was optimized to avoid surface reflections.

DIC software: CORRELI. We used the CORRELI DIC research software developed at the LMT laboratory of ENS Paris-Saclay (France) and implemented in MATLABTM.²⁷ The finite-element software estimates bi-dimensional displacement fields and uses an elastic equilibrium gap regularization. The aim of this procedure is to find the 2D mechanical transformation needed to register images of injected plates onto a reference geometry (mold cavity), based on gray levels from respective images. Subsequently, the full displacement field is obtained over the whole plate surface. The strain field is determined by numerical differentiation of the displacement field.

Digital Image Correlation is mostly used to achieve displacement field measurement during mechanical testing, where a speckle pattern follows the material movement. The principle is based on marks (patterns) matching in accordance with their similarity. The similarity measure is computed globally as a sum of gray level differences over all pixels. Let us emphasize that

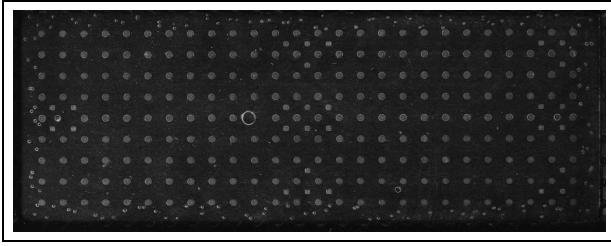


Figure 5. Example of plate image with application of chalk powder.

sub-pixel accuracy requires a gray level interpolation scheme from that of the neighboring pixels. Nevertheless, the DIC method suffers from some limitations. At first, inhomogeneous contrast and brightness differences between the two images to be registered may induce an unsuited measure of similarity. Very sharp contrasts may lead to sub-pixel interpolations that cannot be safely trusted. Moreover, on images, each pixel is affected by noise having several origins (photon, readout electronics, thermal...) leading to displacement uncertainties. Pixels at the edges of the region of interest are also critical since information is poorer in these locations than in the central part and can lead to convergence difficulties at image edges. Finally, the regularization strategy, which is used in the bulk, is much less reliable along edges.

Regarding the use of CORRELI software, a region of interest was first defined on the reference image. This region was delimited to a surface of 5780×2110 pixels, that is $273.1 \times 99.7 \text{ mm}^2$. Inside this region, a mesh area is selected onto which the displacement field is decomposed using bi-linear triangular finite-elements (T3 elements)²⁸ (Figure 6(a)). The mesh size is chosen to be small enough not to be limiting in terms of kinematics (here triangles have a typical edge length of 80 pixels for the reported results in the following). The mesh grid, defined on surface of 5630×2050 pixels and composed of 1860 nodes, is also used to enforce a smoothness of the displacement field based on regularization. An elastic equilibrium gap kernel was used in the following, which acts as a low-pass filter on the displacement field, below a chosen characteristic length scale that effectively sets the spatial resolution, when it is much larger than the element size. A maximum iteration number of 50 was chosen, together with a convergence criterion of $1.0E^{-6}$, as a norm of mean displacement correction between consecutive iterations. Sub-pixel gray level interpolation is chosen as linear or cubic. Finally, an overall brightness and contrast correction is performed over the entire image to provide the needed correspondence between mold and part gray levels. After convergence, the output is the displacement field for registering the two images, as well as the “residual field” (Figure 6(b)) which is the final difference in gray levels after registration. The norm of this field is the quantity, which is minimized for registration, and the residual field shows

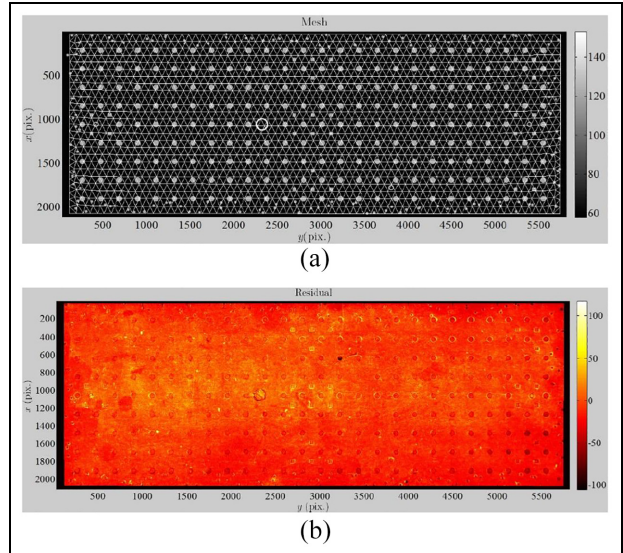


Figure 6. (a) Region of interest mesh on the generated mold image and (b) residual field at correlation calculation convergence for the reference plate. Mesh and residual scales are in pixels; X coordinates (vertical downward) and Y coordinates (horizontal rightward) are in pixels.

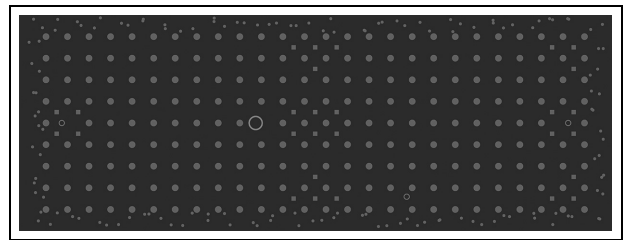


Figure 7. Mold image generated from CAD geometry with a Python script.

what cannot be explained by a mere pixel translation and is a measure of the quality of the registration. Once all the parameters are defined, the correlation procedure is quite fast compared to former techniques since it takes only about 10 min for the calculation to converge with this image quality and to obtain in-plane shrinkages fields over the entire injected part.

Generation of a reference image for DIC technique. In the first steps of the study, a photography of the mold surface was used as a reference image. However, high light intensity variation on the metallic mold surface, parasitic reflection on the shiny surface of the mold generated highly inhomogeneous brightness and contrast variation along the surface (as well as a significant level of noise). Then, a mold image generated from CAD geometry was used for every correlation analysis (Figure 7). The image was generated with a Python script and has a pixel size of $47.25 \mu\text{m}$. Contrary to the mold image, the generated image does not have optical distortions induced by the camera, present no light

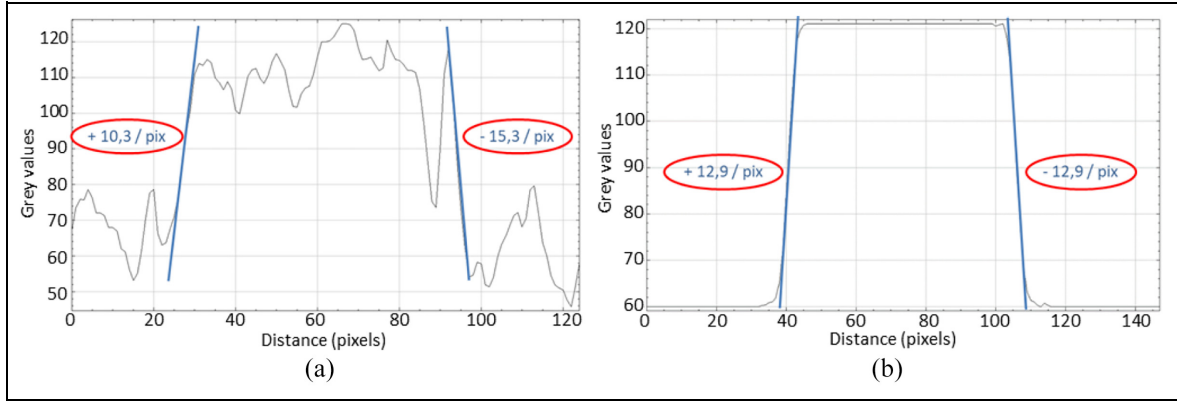


Figure 8. Comparison of gray level variation at engraving transition between (a) an injected plate image and (b) the Gaussian filtered CAD image.

reflection and has a perfect geometry, strictly corresponding to mold geometry, where engravings were machined with a positioning uncertainty lower than 0.01 mm. The measured deformation of the entire surface between the generated image and a mold image achieved by DIC has a standard deviation below 0.03%. This value is considered as the final uncertainty of our experimental setup.

To enhance the correlation convergence, specific gray levels were applied, corresponding to those identified on injected plate images with a mere affine correspondence of gray levels. At this stage, the mold image is binary. A Gaussian filter was applied on the generated image to optimize the sub-pixel interpolation of gray level at each mark boundary (the only exploitable information for DIC) (Figure 8).

To test the sensitivity of the CORRELI software on the marking density, synthetic images were generated thanks to a Python script and compared with images having artificially imposed in-plane longitudinal and transverse shrinkages of 1%. The aim of this procedure is to evaluate the effect of an increase in engravings density (Figure 9(b)) and the effect of a speckle pattern (Figure 9(c)) on the measurement dispersion of in-plane shrinkages.

For the image with randomly dispersed circles, boxes of 100×100 pixels were defined, each containing one randomly located disk of diameter ranging from 10 to 33 pixels. Thus, the whole generated image is composed of 1064 disks, with a density of 3.9 cm^{-2} .

For the image with the speckle pattern, a random field of 275×100 pixels was first generated with a random gray level for each pixel. Thanks to a cubic spline interpolation (python function *interpolate.interp2d*), a 20 times finer pixel field was computed resulting in a 5500×2000 pixels image, shown in Figure 9(c), with spots of approximately 1 mm size.

Thus, three images presenting different marks density were compared:

-1 cm^{-2} for the present mold image with additional random disks on the edges;

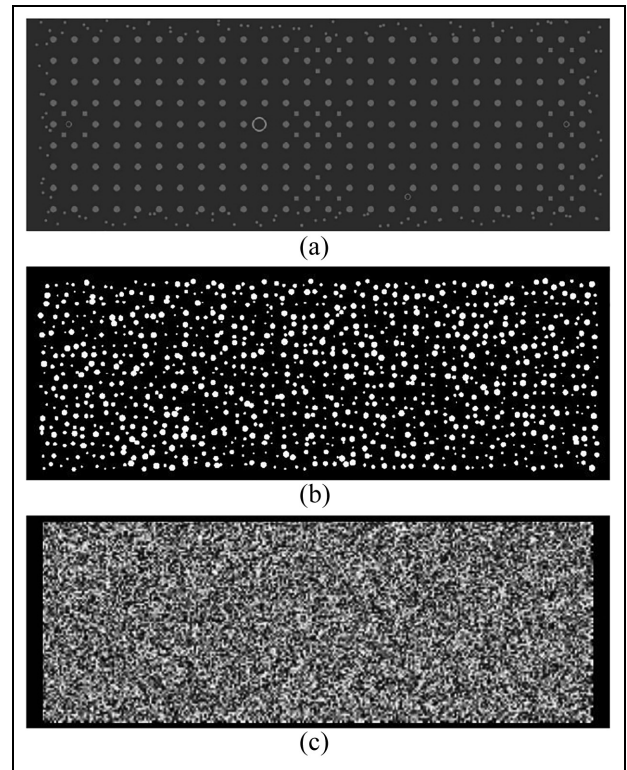


Figure 9. Generated images for sensitivity tests of DIC software with (a) engravings from mold cavity, (b) randomly dispersed circular engravings, and (c) speckle pattern.

-3.9 cm^{-2} for the image with randomly dispersed disks;
 $-\text{about } 100 \text{ cm}^{-2}$ for the random speckle pattern.

Results and discussion

Preliminary study: Marking sensitivity test for DIC

Three images of mold image generated by python scripts and presenting different marks density were created (§2.3.5), a copy of each of them was created by applying 1% shrinkages in both in-plane directions (i.e. flow and transverse). For the three image pairs, DIC

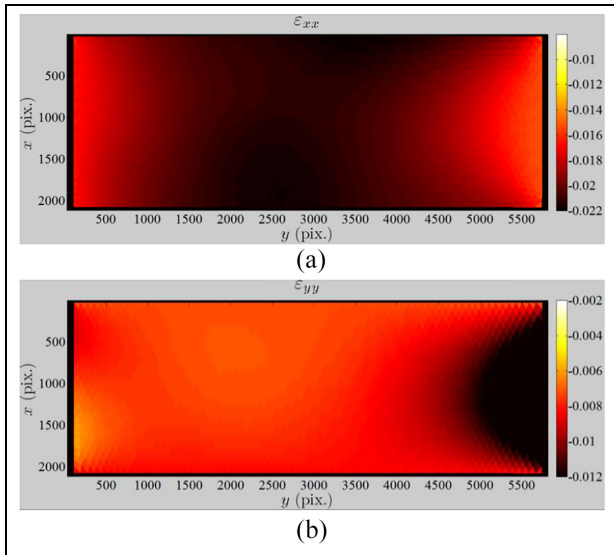


Figure 10. In-plane shrinkages field in (a) transverse direction and (b) flow direction. Shrinkage value scales are dimensionless, X coordinates (vertical downward) and Y coordinates (horizontal rightward) are in pixels.

analyses were launched on CORRELI to evaluate the dispersion of strain measurements according to marks density.

For the image created from the CAD geometry of the mold surface, in-plane shrinkages were determined with a standard deviation of 0.02% (200 $\mu\epsilon$) on the entire surface. For the image with randomly dispersed circles, these 1% in-plane shrinkages have a standard deviation of 0.006% (60 $\mu\epsilon$), more than three times less. Thus, multiplying by 4 the density of marking on the reference image, and increasing the mean of gray level gradient, made the shrinkage dispersion reduced by the same order of magnitude. Lastly, the effect of speckle pattern, as often used for DIC analyzes, provided, as expected, the most consistent results with a standard deviation for shrinkage measurements of only 0.0001% (1 $\mu\epsilon$), showing that refining the density of marking has a roughly linear influence on the precision of in-plane shrinkages measurement. Such an influence of speckle size (i.e. marking density) on displacement measurement resolution has already been observed²⁹ and has to be cautiously considered with respect to pixel size in order not to induce a poor pixel sampling of the gray level distribution.

To conclude on this preliminary study, the pattern and density of marking on the mold cavity is sufficient to measure part in-plane shrinkages, with a standard deviation of 0.02%. However, it may be emphasized that the addition of small engravings on mold cavity edges helped the DIC code to provide trustworthy results in these areas. Indeed, the standard deviation for edges is 1.3 higher than the one for the rest of the surface for the image surface with randomly dispersed circles. For the generated mold image, an increase in standard deviation by a factor of only 1.2 is due to the addition of the small engravings on mold edges.

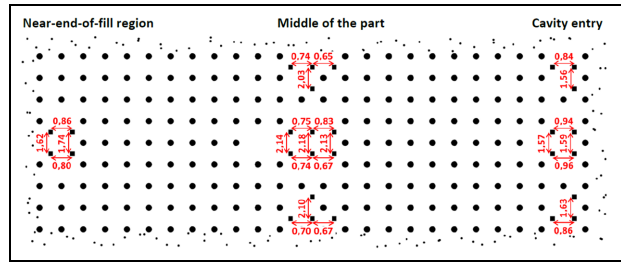


Figure 11. Longitudinal and transverse shrinkage measurements (in %) on biocomposite parts injected at 30 mm/s without packing pressure.

Shrinkage field measurement with DIC methodology

Reference case: The simple plate without packing pressure. The reference case of the study consists of a simple plate injected with a fan gate at a constant ram speed of 30 mm/s without packing pressure. From Figure 10(a), transverse shrinkage can be seen to reach values higher than 2% in the central part of the plate. Left and right plate ends show a smaller shrinkage, ranging between 1.6% and 1.7%, which is imputable to geometrical constraints at cavity corners and to a more extensional flow in these areas. In the flow direction, shrinkage values range from 0.7% to 0.8%, inducing an anisotropic shrinkage ratio ranging from 2.5 to 3. The effect of flow-oriented fibers can be clearly observed. This ratio remains in a similar value range for all other injection conditions tested in the present study and is in agreement with thermal conduction coefficient measurements achieved in both flow and transverse directions on the bio-composite in a former study.²⁶

On longitudinal shrinkage field (Figure 10(b)), a highly shrunk area at cavity entry is visible, showing values exceeding 1.2%, revealing an unexpected increase in shrinkage of a factor of 1.5 as compared to most of the part. This highly shrunk area illustrated on Figure 10(b) has a longitudinal extent of 40 mm. It is the part of the cavity mainly filled with the polymer, which entered the cavity last, thus the warmest area. At the end of filling, the surrounding lateral edges and gate are solidifying quicker than this area. This later solidification in the inner area may result in more strain at the end of part cooling in the longitudinal direction. In addition to this phenomenon, a molten material back-flow may occur due to the delay between the injection ram stop and the valve gate closing at switchover.

We can notice a good agreement between the DIC results and the profilometry measurements (Figure 11). However, profilometry is much less precise and some discrepancies exist due to higher warpage, large off-plane deformations impact in-plane measurement by profilometry. Besides, the lack of a subsequent packing pressure and an early part/mold detachment at cooling lead to less pronounced engravings. These results illustrate the benefit of measuring full-field shrinkages of

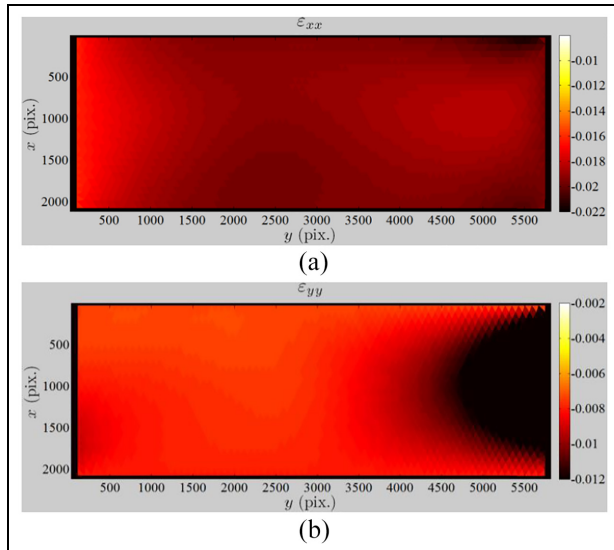


Figure 12. In-plane shrinkage field in (a) transverse and (b) flow direction for a plate injected with a tab gate.

injection molded polymer plates instead of performing local measurements, as for profilometry, where the high shrinkage area at cavity entry is not well captured (Figure 3).

In transverse direction, the trend observed in the DIC results is also found by profilometry, that is a maximum transverse shrinkage in the middle of the part with values exceeding 2%.

Effect of injection gate type. Using a tab gate instead of a fan gate decreases the anisotropy of in-plane shrinkages with mainly a decrease in transverse shrinkage (Figure 12). Indeed, without packing pressure, a high longitudinal shrinkage, exceeding 1.2%, is also visible at cavity entry due to the surrounding geometrical constraints with mold walls and injection gate. Moreover, the area size affected by high longitudinal shrinkage is still extended compared to the reference case, due to the extensional flow, which tends to homogenize in-plane shrinkages.

This strong spatial effect of gate can be evidenced experimentally only by such a full-field measurement.

Effect of ram speed. The increase in injection velocity from 30 to 100 mm/s has a limited effect on in-plane shrinkages (Figure 13). However, they are paradoxically lower for the highest velocity. Typically, at higher injection velocities, the thickness of the solidified layer during filling is decreased since less time is let to the polymer to solidify at mold interface. Thus, it is expected to lead to higher in-plane shrinkages. This trend is not observed between Figures 10 and 13 and a more consequent inertia effect of the injection screw at higher velocities may be suspected.

Effect of geometrical constraint. Plates with added peripheral ribs shows lower in-plane shrinkages compared to

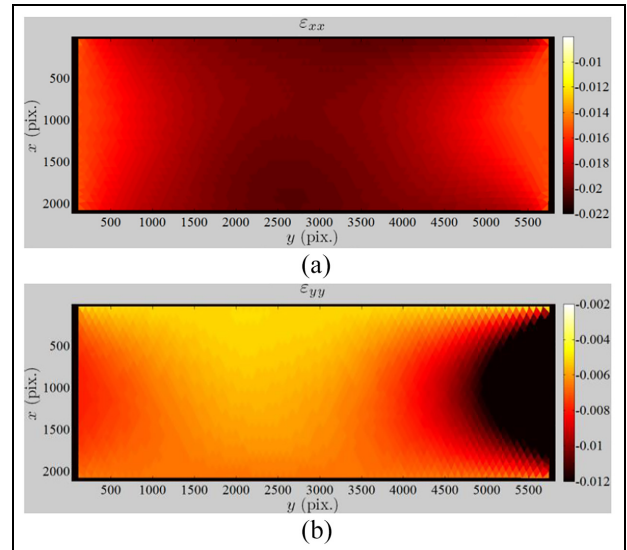


Figure 13. In-plane shrinkage field in (a) transverse and (b) flow direction for a ram speed of 100 mm/s.

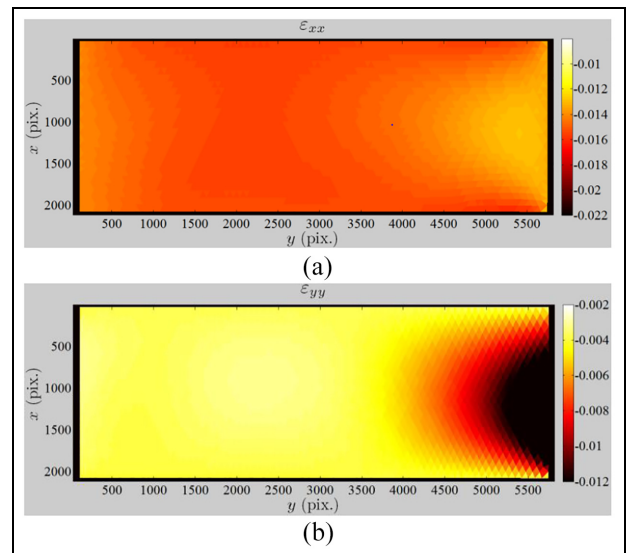


Figure 14. In-plane shrinkages field in (a) transverse direction and (b) flow direction for a plate injected with peripheral ribs.

the simple plate configuration, confirming that stress relaxation occurred during cooling in the mold with a small decrease in thickness. Nevertheless, the thickness variation is too small to precisely calculate a shrinkage in thickness direction and then a volumetric shrinkage that should not vary. In the transverse direction, shrinkage is more homogeneous than that of the simple plate configuration, with a decrease in shrinkage values by 0.5 % in the center of the part (Figure 14(a)). At cavity entry, a higher shrinkage gradient can be noticed on the periphery of the plates due to the ribs.

In the longitudinal direction (Figure 14(b)), shrinkage is reduced by 0.2 % as compared to the reference case at the exception of the highly shrunk area. This area at cavity entry is still visible without a post-filling

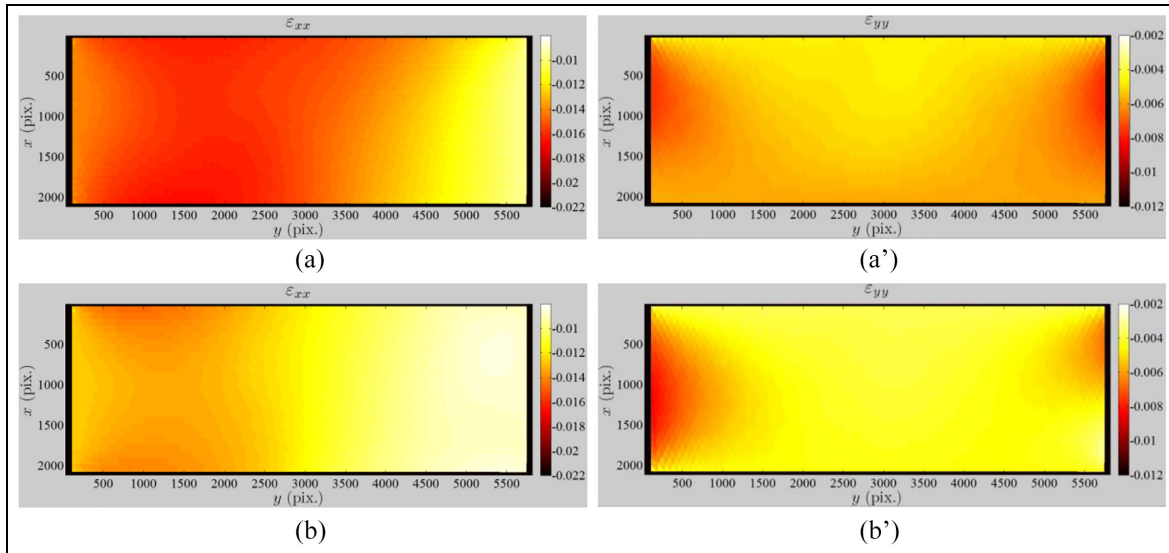


Figure 15. (a, b) and (a', b'): transverse (left column) and along flow (right column) shrinkage field for packing phase of respectively 30 MPa (top row) and 40 MPa (bottom row).

phase but is affected by the peripheral ribs, with a smaller extent of 28 mm.

Effect of packing pressure on shrinkage anisotropy. The shrinkage fields of two packing pressure levels were studied: 30 (Figure 15(a) and (b)) and 40 MPa (Figure 15(a') and (b')) applied at the nozzle during 10 s. The first visible effect of packing pressure is the decrease in longitudinal shrinkage level for 30 MPa with shrinkage values ranging from 0.5% to 0.6%, and shrinkage values ranging from 0.4% to 0.5% for 40 MPa. Besides, the area with high shrinkage at cavity entry, observed in Figure 10(b) for the reference case, tends to disappear and is even inexistent for a pressure of 40 MPa (Figure 15(b')). The packing pressure compensates material volumetric shrinkage, especially at the cavity entry.

As in the reference case without packing pressure (Figure 10(a)), an area with highest transverse shrinkage is visible for both cases with packing pressure. However, the position of this area tends to move toward near-end-of-fill as the packing pressure increases. This shift of shrinkage position illustrates the effect of packing pressure which is stronger near the injection gate where a large amount of polymer is still at molten state at the end of cavity filling.

The profilometry measurements again confirm the in-plane shrinkages levels (Figure 16) comparable to those calculated by DIC.

How to compare DIC experimental measurements with simulation results?

Developing a methodology to accurately measure in-plane shrinkage field allows the process simulation to be validated against experimental measurements.

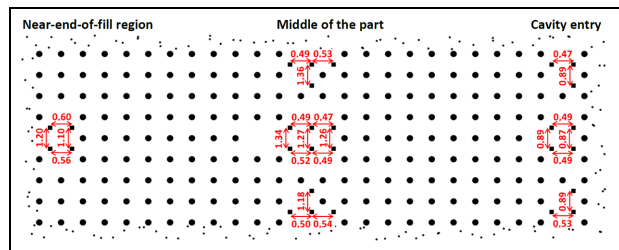


Figure 16. Longitudinal and transverse shrinkage measurements (in %) on biocomposite parts injected at 30 mm/s with packing pressure.

Predictions of full-field shrinkages induced by varying injection conditions are confronted with the experimental measurements obtained by DIC. The best set of parameters of the material constitutive equations is then identified, based on the quality of part shrinkage prediction. This parameter identification optimization is the condition to shift to an industrial part presenting a more complex 3D geometry.

The simulations were performed on the commercial simulation code Autodesk Moldflow Insight 2019. The warpage analysis, which constitutes the last step of simulation, provides the computed full-field strain of an injection molded polymer plate in specific conditions (Figure 17(a) and (b)). With the developed methodology and the use of the open-source platform ParaView, we can confront these simulation results to the measured full-field shrinkages for the same injection conditions (Figure 17(a) and (b')). For this example of process conditions (simple plate injected at 30 mm/s with the tab gate and a packing pressure of 40 MPa), we can notice that shrinkage field in transverse direction is very well predicted by the simulation code (Figure 17(a)). This is however to be contrasted with the flow direction, where simulated shrinkage is largely

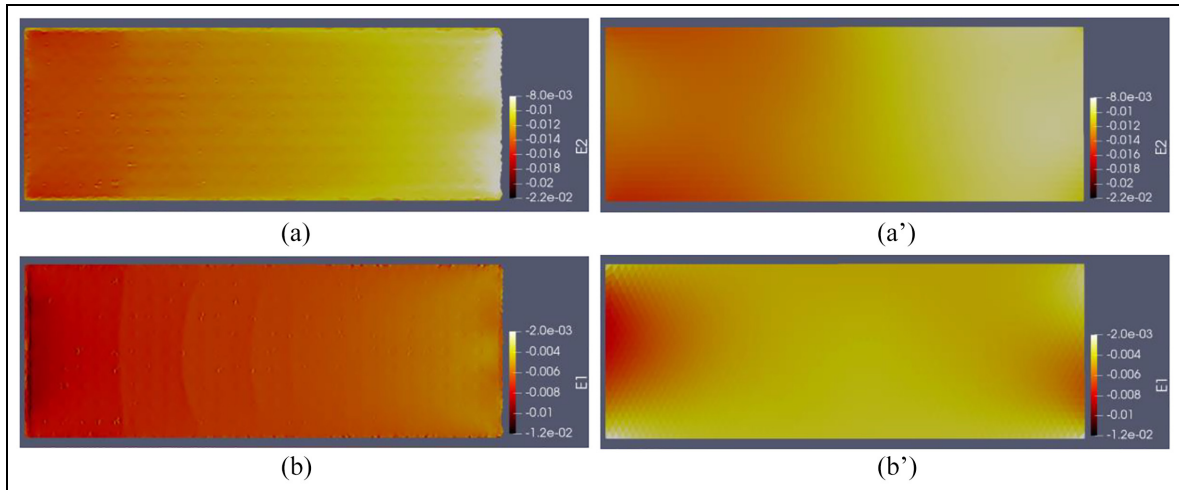


Figure 17. (a, a') and (b, b'): Simulated (left column) and measured (right column) shrinkage fields comparison for the injection molded simple plate with tab gate and a packing pressure of 40 MPa for respectively transverse (top row) and flow (bottom row) directions.

overestimated (Figure 17(b)), twice as large as the measured one.

The observed gap can be explained by numerous reasons, such as a poor prediction of fiber distribution and orientation,²⁶ no stress relaxation being taken into account during cooling or a too simple “no-flow” condition depending only on temperature. The present DIC approach gives the opportunity to finely identify the material behavior or characterization so that simulated and measured in-plane shrinkage fields coincide at best. Once this fine identification achieved, other simulation procedures can be launched on more complex 3D geometries, so as to observe if the correction of material parameters is efficient for more complex material flows.

Conclusion

Correct prediction of shrinkage and deformation of injection-molded parts still remains a first-rate technical and scientific challenge, considering the high cost of processing tools. This is even more true as new composite materials are appearing on the market. Such is the case for instance for newly developed polymers reinforced with natural fibers, whose fine characterization is more complex. For this reason, a new methodology based on Digital Image Correlation (DIC) has been proposed to measure full-field in-plane shrinkage on injection molded plates and to directly offer the possibility to compare simulations and measurements.

The proposed method is based on the registration of a mold surface and a molded plate by DIC. The use of DIC requires small marks or engravings to be machined on the metallic mold surface in order to modify the roughness of the surface, and therefore the local brightness, contrast and gray level on images of the plates. Small-engraved disks can be easily performed by Electrical Discharge Machining process (EDM). Their

surface should be large enough to create significant local contrast, a diameter of 1 mm on a depth of a few tens of microns was shown to be a minimum for the size of the analyzed surface. The chosen engraving density and pattern allow for in-plane shrinkage measurements with a sufficient strain measurement uncertainty (standard deviation of 0.03%). This uncertainty was shown to vary roughly linearly with the marking density. However, it was highly beneficial to increase the marking density along the edges to mitigate the lack of kinematic constraints for DIC along boundaries. Last, the good geometrical quality of the bench for image capture should be considered carefully.

The DIC methodology presents a fast and robust approach for measuring full-field shrinkage on large rectangular injected parts in less than 10 min for the numerical treatment with CORRELI DIC software. It showed enough sensitive to distinguish quantitatively in-plane shrinkages between two close injection conditions like packing pressures of 30 and 40 MPa. The spatial effect of added geometrical constraints on plates, which prevents (or not) the plate slippage during the cooling in the mold, that is the stress relaxation, were very clearly revealed and quantified.

This sensitive in-plane shrinkage measurement methodology is expected to be extensively used to calibrate and improve the prediction of part shrinkage and warpage by rheological finite-elements simulation. It allows comparing quite easily full-field in-plane shrinkage measurements and their numerical simulation, then the identification of the physical characterization of a material, of its thermomechanical behavior or of the nature of boundary conditions can be performed much more precisely and trustfully. Finally, through a better-validated digital twin of the injection process, optimization of molding for the existing and even more so for new materials is offering very appealing perspectives.

CRedit authorship contribution statement

Antoine Dupuis: Conceptualization, methodology, software, validation, formal analysis, investigation, data curation, writing – original draft, writing – review and editing, visualization. Jean-Jacques Pesce: Methodology, validation, resources, supervision, project administration, funding acquisition. Jean-Baptiste Marijon: Software, investigation, data curation. Stéphane Roux: Software, validation, writing – review and editing. Gilles Régnier: Conceptualization, methodology, validation, formal analysis, writing – review and editing, visualization, supervision, project administration, funding acquisition.

Declaration of conflicting interests

The author(s) declared no potential conflicts of interest with respect to the research, authorship, and/or publication of this article.

Funding

The author(s) disclosed receipt of the following financial support for the research, authorship, and/or publication of this article: The authors wish to acknowledge the *Association Nationale Recherche Technologie* (ANRT), France, based on the decision number 2017/1103 and Faurecia company for funding this research work.

ORCID iDs

Antoine Dupuis  <https://orcid.org/0000-0003-1879-9888>

Jean-Baptiste Marijon  <https://orcid.org/0000-0003-4358-0159>

Stéphane Roux  <https://orcid.org/0000-0003-4885-6732>

Gilles Régnier  <https://orcid.org/0000-0002-1543-1837>

References

1. Kennedy PK. *Practical and scientific aspects of injection molding simulation*. Eindhoven: Technische Universiteit Eindhoven, 2008. <https://doi.org/10.6100/IR634914>
2. Bushko WC and Stokes VK. Solidification of thermoviscoelastic melts. Part II: effects of processing conditions on shrinkage and residual stresses. *Polym Eng Sci* 1995; 35: 365–383.
3. Santis FD, Pantani R, Speranza V, et al. Analysis of shrinkage development of a semicrystalline polymer during injection molding. *Ind Eng Chem Res* 2010; 49: 2469–2476.
4. Jansen KMB, Van Dijk DJ and Husselman MH. Effect of processing conditions on shrinkage in injection molding. *Polym Eng Sci* 1998; 38: 838–846.
5. Pomerleau J and Sanschagrin B. Injection molding shrinkage of PP: experimental progress. *Polym Eng Sci* 2006; 46: 1275–1283.
6. Delaunay D, Le Bot P, Fulchiron R, et al. Nature of contact between polymer and mold in injection molding. Part II: influence of mold deflection on pressure history and shrinkage. *Polym Eng Sci* 2000; 40: 1692–1700.
7. Leo V and Cuvellez C. The effect of the packing parameters, gate geometry, and mold elasticity on the final dimensions of a molded part. *Polym Eng Sci* 1996; 36: 1961–1971.
8. Delaunay D, Le Bot P, Fulchiron R, et al. Nature of contact between polymer and mold in injection molding. Part I: influence of a non-perfect thermal contact. *Polym Eng Sci* 2000; 40: 1682–1691.
9. Kmetty A, Tabi T, Kovacs JG, et al. Development and characterisation of injection moulded, all-polypropylene composites. *Express Polym Lett* 2013; 7: 134–145.
10. Régnier G and Trotignon JP. Local orthotropic shrinkage determination in injected moulded polymer plates. *Polym Test* 1993; 12: 383–392.
11. Jansen KMB. Measurement and prediction of anisotropy in injection moulded PP products. *Int Polym Process* 1998; 13: 309–317.
12. Speranza V, Vietri U and Pantani R. Monitoring of injection moulding of thermoplastics: adopting pressure transducers to estimate the solidification history and the shrinkage of moulded parts. *Stroj Vestn – J Mech Eng* 2013; 59: 677–682.
13. Masato D, Rathore J, Sorgato M, et al. Analysis of the shrinkage of injection-molded fiber-reinforced thin-wall parts. *Mater Des* 2017; 132: 496–504.
14. Sutton M, Wolters W, Peters W, et al. Determination of displacements using an improved digital correlation method. *Image Vis Comput* 1983; 1: 133–139.
15. Chevalier L, Calloch S, Hild F, et al. Digital image correlation used to analyze the multiaxial behavior of rubber-like materials. *Eur J Mech A Solids* 2001; 20: 169–187.
16. Hild F, Raka B, Baudequin M, et al. Multiscale displacement field measurements of compressed mineral-wool samples by digital image correlation. *Appl Opt* 2002; 41: 6815–6828.
17. Neggers J, Hoefnagels JPM, Geers MGD, et al. Time-resolved integrated digital image correlation. *Int J Numer Methods Eng* 2015; 103: 157–182.
18. Hild F and Roux S. Digital image correlation: from displacement measurement to identification of elastic properties - a review. *Strain* 2006; 42: 69–80.
19. Gershon AL, Gyger LS, Bruck HA, et al. Thermoplastic polymer shrinkage in emerging molding processes. *Exp Mech* 2008; 48: 789–798.
20. Chuang SF, Chen TY and Chang CH. Application of digital image correlation method to study dental composite shrinkage. *Strain* 2008; 44: 231–238.
21. Li JY, Lau A and Fok ASL. Application of digital image correlation to full-field measurement of shrinkage strain of dental composites. *J Zhejiang Univ Sci A* 2013; 14: 1–10.
22. Kravchenko OG, Kravchenko SG, Casares A, et al. Digital image correlation measurement of resin chemical and thermal shrinkage after gelation. *J Mater Sci* 2015; 50: 5244–5252.
23. Motagi S, Namilae S, Freeman T, et al. In-situ measurement of resin shrinkage with respect to degree of cure. In: *AIAA Scitech 2020 forum*, Orlando, FL, 6 January 2020. Reston, VA: American Institute of Aeronautics and Astronautics.
24. Sun X, Zeng D, Tibbenham P, et al. A new characterizing method for warpage measurement of injection-molded thermoplastics. *Polym Test* 2019; 76: 320–325.
25. Yang Y, Yang B, Zhu S, et al. Online quality optimization of the injection molding process via digital image processing and model-free optimization. *J Mater Process Technol* 2015; 226: 85–98.

26. Dupuis A, Pesce J-J, Ferreira P, et al. Fiber orientation and concentration in an injection-molded Ethylene-Propylene copolymer reinforced by Hemp. *Polymers* 2020; 12: 2771.
27. Hild F and Roux S. Digital image correlation. In: Rastogi P and Hack E. eds (eds) Chap. 5. *Optical methods for solid mechanics: a full-field approach*. Weinheim, Germany: Wiley-VCH, 2012, pp.183–228.
28. Hild F and Roux S. Comparison of local and global approaches to digital image correlation. *Exp Mech* 2012; 52: 1503–1519.
29. Bornert M, Brémand F, Doumalin P, et al. Assessment of digital image correlation measurement errors: methodology and results. *Exp Mech* 2009; 49: 353–370.